ARTICLE

Age-differential CD13 and interferon expression in airway epithelia affect SARS-CoV-2 infection - Effects of vitamin D

Francesca Sposito [1], Shaun H. Pennington [2], Christopher A.W. David [3], Jack Duggan [2], Sarah Northey [1], Giancarlo A. Biagini [2], Neill J. Liptrott [3], Amandine Charras [1], Paul S. McNamara [1,4,†] and Christian M. Hedrich [1,5,✉,†]

Young age and high vitamin D plasma levels have been associated with lower SARS-CoV-2 infection risk and favourable disease outcomes. This study investigated mechanisms associated with differential responses to SARS-CoV-2 across age groups and effects of vitamin D.

Nasal epithelia were collected from healthy children and adults and cultured for four weeks at the air-liquid interface with and without vitamin D. Gene expression and DNA methylation were investigated. Surface protein expression was confirmed by immunofluorescence while vitamin D receptor recruitment to the DNA was analysed through chromatin immunoprecipitation. HEp-2 cells were used for protein co-immunoprecipitation and luciferase reporter assays.

Compared to children, airway epithelia from adults show higher viral RNA recovery following infection. This was associated with higher *ANPEP*/CD13, reduced type I interferon expression, and differential DNA methylation. In cells from adults, exposure to vitamin D reduced TTLL-12 expression, a negative regulator of the interferon response. This was mediated by vitamin D receptor recruitment to *TTLL12*, where it instructs DNA methylation through DNA methyltransferase 1.

This study links age-dependent differential expression of CD13 and type I interferon to variable infection of upper airway epithelia. Furthermore, it provides molecular evidence for vitamin D reducing viral replication by inhibiting TTLL-12.

INTRODUCTION

Severe Acute Respiratory Syndrome Coronavirus 2 (SARS-CoV-2), a betacoronavirus responsible for the COVID-19 pandemic, has caused millions of deaths worldwide[1,2]. Population and individual host factors influence disease severity, with age, ethnicity, and socioeconomic status as key factors determining outcomes[1,3]. Notably, most children and young people (<18 years) experienced milder disease severity during the pandemic or were asymptomatic. However, the exact reasons for this remain unclear[1,3].

In addition to SARS-CoV-2, the *Coronaviridae* family includes Middle East Respiratory Syndrome-related Coronavirus (MERS-CoV), SARS-CoV, and the seasonal HCoV-229E. The majority of coronaviruses transmitted among humans originate from bats[4]. They infect cells through membrane proteins such as angiotensin-converting enzyme 2 (ACE2) or peptidases[4,5]. SARS-CoV-2 binds ACE2 and enters the cell following priming through transmembrane serine protease 2 (TMPRSS2) in a process facilitated by neuropilin-1 (NRP1)[6,7].

Calcitriol, or 1α,25-dihydroxyvitamin D_3, has immunomodulatory effects and may protect against viral airway infections[8–11]. Low vitamin D plasma levels (<20 ng/mL) are more common in elderly populations and can be associated with socioeconomic disadvantage[12,13]. Epidemiological studies suggest that individuals with low vitamin D plasma levels experience more severe COVID-19 and poorer outcomes[9,14]. There have been few studies to date on the role of calcitriol in COVID-19, but in other conditions, it alters gene expression in immune and airway epithelial cells[15]. Calcitriol binds to the vitamin D receptor (VDR), a nuclear transcription factor. This complex then migrates to the cell nucleus, where it binds to vitamin D response elements, and induces epigenetic remodelling, including DNA methylation[15]. These epigenetic modifications regulate chromatin accessibility to transcription factors and RNA polymerases without altering the underlying DNA sequence[16].

The aim of this study was to identify molecular mechanisms associated with milder COVID-19 severity in children and young people (CYP) compared to adults and the possible impact of vitamin D on epithelial immune responses to SARS-CoV-2, using

† Both authors contributed equally to this work.

[1]Department of Women's & Children's Health, Institute of Life Course and Medical Sciences, University of Liverpool, Liverpool, UK. [2]Centre for Drugs and Diagnostics, Department of Tropical Disease Biology, Liverpool School of Tropical Medicine, Liverpool, UK. [3]Immunocompatibility Group, Department of Pharmacology and Therapeutics, Institute of Systems, Molecular, and Integrative Biology, University of Liverpool, Liverpool, UK. [4]Department of Respiratory Medicine, Alder Hey Children's NHS Foundation Trust Hospital, Liverpool, UK. [5]Department of Paediatric Rheumatology, Alder Hey Children's NHS Foundation Trust Hospital, Liverpool, UK. ✉ email: christian.hedrich@liverpool.ac.uk

an established primary human upper respiratory epithelium model.[17]

RESULTS

SARS-CoV-2 RNA recovery is greater in airway epithelia from adults compared to CYP prior to infection

We evaluated the ability of SARS-CoV-2 to infect and replicate in primary human airway epithelial cells (AECs) from CYP (<18 years) and adults (>50 years) *in vitro* by quantifying viral RNA in cell supernatants 48 hours after infection. When compared to cells from CYP, viral RNA recovery was higher in AECs from adults (3.25×10^5 vs. 4.83×10^5 copies/μL, p < 0.01, Fig. 1). No differences were detected in viral replication between young children (median age: 9 months, range: 7–23 months) and young people/adolescents (median age: 11 years, range: 10–14 years) (Supplementary Fig. 2).

SARS-CoV-2 recovery associates with CD13 expression

To determine whether age-related differential gene expression in AECs promotes infection and/or virus replication, we analysed the mRNA expression of >700 genes using the NanoString host response panel, including additional custom probes for ACE2 isoforms (Fig. 2, Supplementary Fig. 3). While we did not detect differences in the expression of *ACE2*, *TMPRSS2*, and *NRP1* (Supplementary Fig. 3), we identified three differentially expressed genes comparing AECs from CYP and adults: CD13 (encoded by *ANPEP*, 0.05 vs. 0.31 fold change, p < 0.001), *HLA-DQA*, and *CXCL-13* (Figs. 2A and 2B). The *ANPEP* gene was of particular interest because its protein product, the alanyl aminopeptidase CD13, had previously been reported as a receptor for seasonal coronavirus infections[18,19]. Thus, we investigated CD13 surface expression and confirmed differential CD13 protein abundance between children and adults, considering surface receptor density and CD13$^+$ AECs (Figs. 2C and 2D).

AECs from children exhibit robust spontaneous type I interferon expression at baseline

The expression of type I interferons (IFNs) and interferon response genes (ISGs) is a key factor of the innate anti-viral response[20,21]. We therefore considered the expression of 30 IFN-related genes included in the NanoString host response panel (Supplementary Methods) and calculated type I IFN scores[22]. Although differences in the expression level of these individual genes in CYP and adults did not reach statistical significance level after correction for false discovery rate (FDR), type I IFN scores were higher in AECs from CYP when compared to adults (0.34 vs. 0.13, p < 0.01, Fig. 3).

DNA methylation associates with age-differential gene expression

Epigenetic patterns change with age while regulating gene expression without altering the underlying DNA sequence[23]. Thus, we examined differential DNA methylation in AECs from CYP and adults using Infinium 850K EPIC methylation arrays (Fig. 4). We identified >29,000 differentially methylated positions (DMPs). Notably, 20,819 (71.8%) were hypermethylated and 8,185 (28.2%) were hypomethylated, cumulatively affecting over 10,000 genes. Some DMPs affected *ANPEP* and genes included in the type I IFN score. A total of 12 CpGs were related to *ANPEP* (Figs. 4B and 4C). Notably, while 8 of 12 CpGs exhibited increased methylation in adults and predominantly localised to
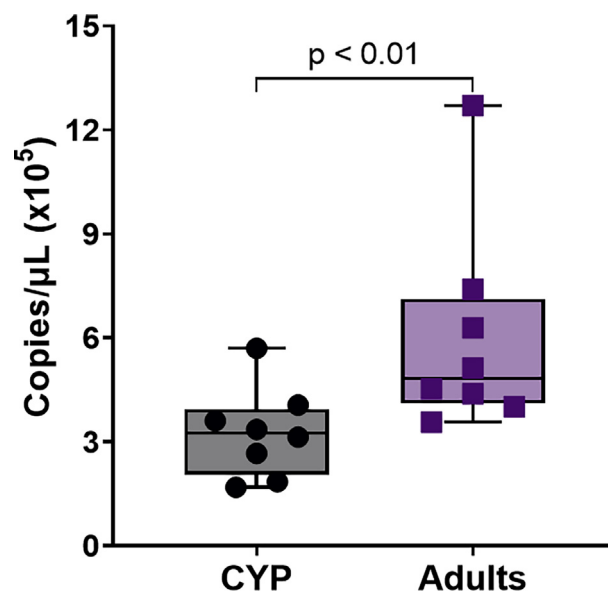
Fig. 1 Age-related differences in SARS-CoV-2 replication in airway epithelial cells. Viral RNA recovery after infection with SARS-CoV-2 was quantified by RT-qPCR. Data are presented as median and interquartile range; statistical significance was tested using the Mann-Whitney test (*n* = 8). CYP = children and young people; RT-qPCR = Quantitative reverse transcription polymerase chain reaction.

the gene body, four CpGs exhibited increased methylation in CYP and were located in the 5′ UTR region.

We then calculated two separate IFN scores using the DNA methylation data: one considering all the beta values of the DMPs in the 30 IFN-related genes (Fig. 4D), and the other considering only the ones in the promoter region of the genes (Fig. 4E). In both cases, CYP shows a higher IFN score compared with adults.

Vitamin D alters DNA methylation and gene expression in airway epithelia from adults prior to infection

Low vitamin D plasma levels (<20 ng/mL) have previously been suggested to associate with increased age, increased risk for severe COVID-19 courses, and poor outcomes[12,13,24]. Thus, we analysed the effects of vitamin D on both DNA methylation and mRNA expression in AECs from CYP and adults (Fig. 5). For this, cell culture media was supplemented with 1α,25-Dihydroxyvitamin D_3 at a concentration of 10^{-9} M or with an equal amount of vehicle solvent. Interestingly, we did not identify differential DNA methylation in AECs from CYP in the absence or presence of vitamin D (Fig. 5A). Conversely, AECs from adults exhibited 12 DMPs comparing AECs in the absence or presence of vitamin D: six CpG positions were hypermethylated and six were hypomethylated (Fig. 5B). One of the most DMP affected the *TTLL12* gene (Fig. 5C), which was associated with differential gene expression (1 vs. 0.8 fold change, p = 0.01, Fig. 5D).

We then investigated whether the treatment with vitamin D impacted viral RNA recovery after SARS-CoV-2 infection. Vitamin D did not have an impact on viral RNA recovery in cells from CYP. In AECs from adults, vitamin D exposure was associated with reduced viral RNA recovery that failed to reach statistical
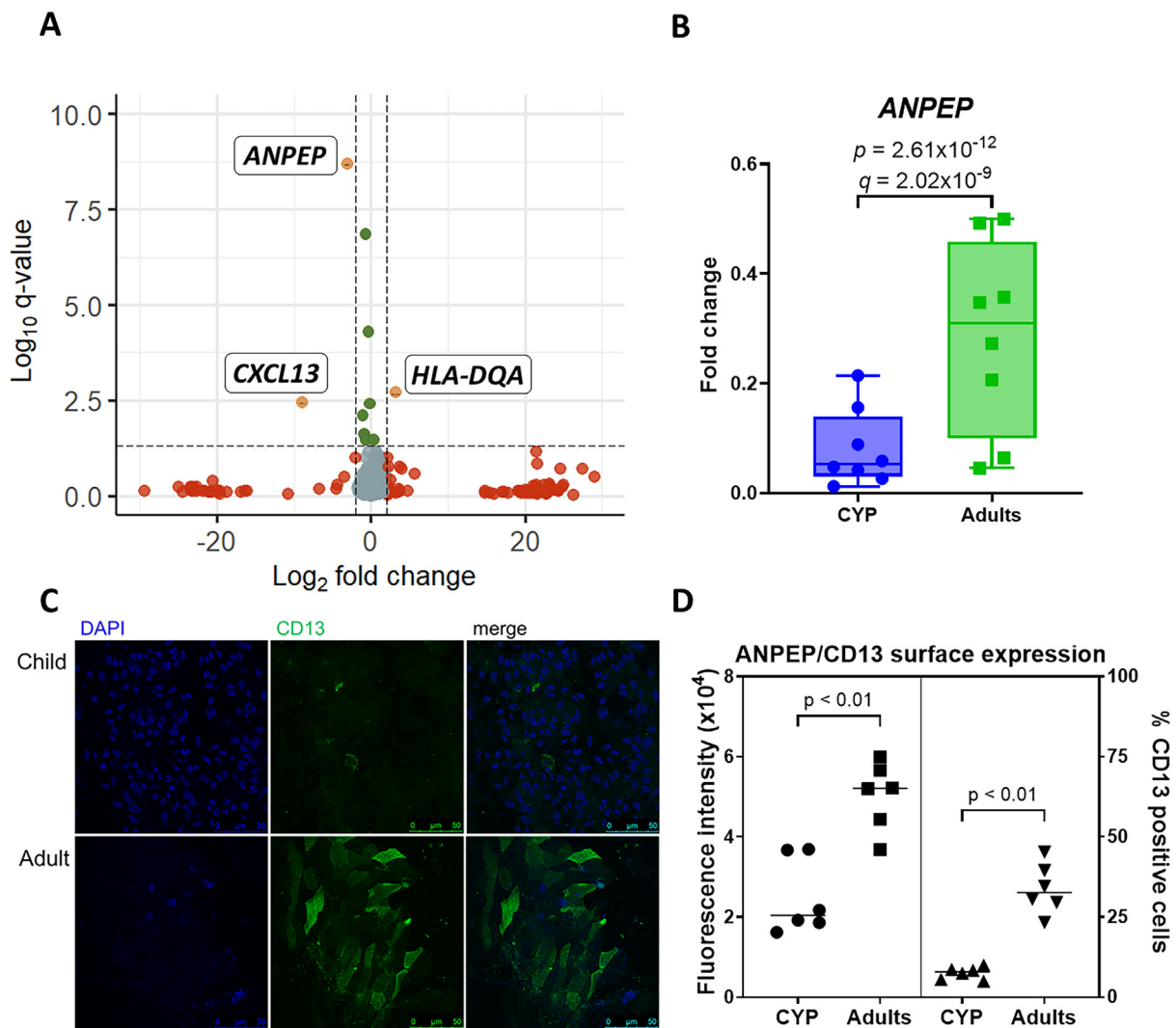
Fig. 2 Airway epithelial cells from adults exhibit increased CD13 expression when compared to children at the baseline. (A) Differentially expressed genes in airway epithelial cells from CYP and adults (p-values were corrected for false discovery rates and referred to as q-values). (B) NanoString gene expression analysis; fold change was calculated as the ratio between the gene counts of the gene of interest and the geometric mean of housekeeping genes counts; data are presented as median and interquartile range (n = 8). CD13 immunostaining (C) and quantification (D); significance was tested using Mann-Whitney test. CYP = children and young people.

significance. Notably, the difference between CYP and adults was lost after the treatment with vitamin D (Fig. 5E).

Vitamin D promotes type I IFN expression in AECs from adults

Previously, TTLL-12 has been suggested to negatively regulate the RIG-I pathway, responsible for type I IFN expression in response to RNA viruses[25]. Thus, we measured type I IFN scores and type I IFN genes expression in AECs from adult donors in the absence or presence of vitamin D. While the type I IFN score, including 30 genes (type I IFNs and ISGs), and ISG expression did not differ (Supplementary Figs. 4 and 5), the expression of individual type I IFN genes was significantly increased in response to treatment with vitamin D (Fig. 6A, Supplementary Fig. 6).

To validate the potential role of TTLL-12, HEp-2 cells were transfected with a pcDNA3.1 expression plasmid carrying the cDNA sequence of *TTLL12* or empty control vectors and calcu-

lated IFN scores (Fig. 6B). In agreement with what was described in the literature, forced expression of TTLL-12 was associated with the reduction of IFN scores[25].

VDR recruitment to *TTLL12* reduces gene expression through epigenetic remodelling

Next, we investigated how vitamin D impacts *TTLL12* expression. To predict regulatory elements upstream of *TTLL12*, we defined highly conserved noncoding sequences (CNS) between mouse and human and mapped predicted consensus VDR binding sites against them[26–28]. This approach delivered two putative VDR binding elements, one in the proximal promoter region of *TTLL12* and one in a 5′ CNS (Fig. 7A). To confirm VDR recruitment to the *in silico* predicted binding elements, we applied chromatin immunoprecipitation (ChIP) followed by semi-quantitative polymerase chain reaction (ChIP-qPCR) (Fig. 7B). Indeed, VDR was recruited to both the predicted binding sites
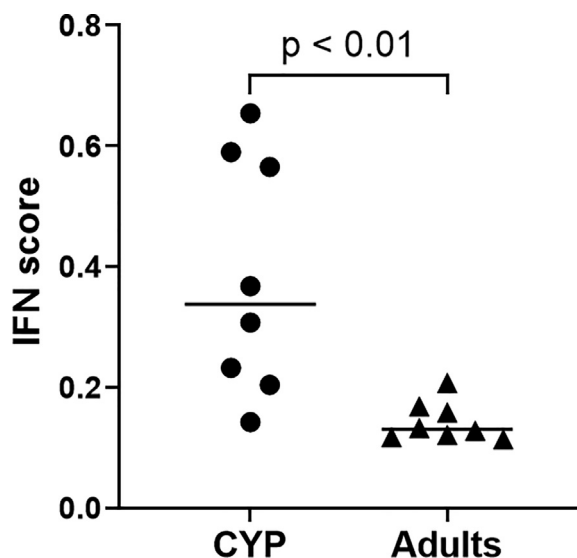
Fig. 3 Age-differential type I interferon expression in airway epithelial cells prior to infection. Type I IFN scores based on the expression of 30 interferon-related genes. Significance was tested using the Mann-Whitney test. CYP = children and young people; IFN = interferons.

upstream of *TTLL12*, which increased in response to vitamin D exposure.

To decipher whether VDR recruitment trans-regulates *TTLL12* expression, we performed luciferase reporter assays applying constructs including the proximal *TTLL12* promoter region (spanning 2.451 bp) or the upstream CNS region including one VDR element (spanning 965 bp). HEp-2 cells were transfected with *Renilla* luciferase plasmids (as a control), empty pGL3 vectors, or luciferase constructs, plus/minus a pcDNA3.1 expression plasmid (with or without the cDNA sequence of *VDR*). After 5 hours of incubation, cells transfected with pGL3 vectors, including the *TTLL12* promoter region, exhibited significantly higher luciferase activity when compared to controls or cells transfected with plasmids, including the CNS region (Fig. 8A). Simultaneous transfection with VDR expression plasmids did not affect the luciferase activity of any of the reporter constructs (Fig. 8B).

As mentioned above, vitamin D exposure altered the DNA methylation of *TTLL12* (Fig. 5C). To understand how VDR recruitment alters DNA methylation, we tested whether VDR physically interacts with DNA methyltransferases (DNMT), namely DNMT 1 and DNMT3A, using protein co-immunoprecipitation (Co-IP) under resting conditions and following forced expression of VDR in HEp-2 cells. Protein quantification through western blot suggested interactions between VDR and both DNMTs (Fig. 8C). To confirm that this interaction is relevant for *TTLL12*, we mapped VDR, DNMT1, and DNMT3A recruitment to the *TTLL12* proximal promoter and the upstream CNS region in HEp-2 cells under resting conditions and after forced expression of VDR, using ChIP. Notably, under resting conditions and especially after VDR over-expression, DNMT1 co-recruited to the *TTLL12* proximal promoter and, to a lesser extent, the upstream CNS element (not reaching statistical significance) (Fig. 8D). This suggests that vitamin D exposure mediates VDR recruitment to *TTLL12*, where it does not result in the trans-regulation of gene expression but controls DNA methylation through interactions with DNMT1 (Fig. 8E).

DISCUSSION

Increasing age associates with a higher risk of symptomatic SARS-CoV-2 infection and severe COVID-19 with increased morbidity, hospitalisation rates, and mortality[3,29,30]. While severe COVID-19 can occur in CYP, it is rare compared to adults and most frequently associated with pre-existing comorbidities[31]. This study provides evidence for molecular mechanisms that underlie this phenomenon. We show increased viral RNA recovery and replication of SARS-CoV-2 in primary AECs from adults compared to CYP. This may allow for a more efficient transition to lower airway involvement and/or systemic disease instead of being cleared in the upper airways. In fact, AECs from CYP exhibited reduced expression of *ANPEP*/CD13 in the presence of increased type I IFNs expression.

The CD13 surface protein is a co-receptor that has previously been linked with seasonal coronavirus infections. The seasonal coronavirus HCoV-229E, through the spike protein that is conserved within the *Coronaviridae* family, recruits to CD13 within so-called lipid rafts, thereby propagating infection[19]. Moreover, increased spontaneous expression of type I interferons and interferon response genes (ISGs), that were quantified as interferon signature, may add another protective layer in CYP. Indeed, increased type I interferon and ISG expression has previously been linked with robust protection from RNA virus infections in airway epithelia[21].

Interestingly, we did not find differences in *ACE2*, *TMPRSS2*, and *NRP1* genes expression when comparing data from CYP and adults. Notably, both the presence and the absence of differential expression of these genes between age groups have previously been reported, and gene expression may differ not only between age groups but also between regions within the respiratory tract[32,33]. In this study, we focused our attention on the upper airways (isolating cells only from nasal brushings), where ACE2, TMPRSS2, and NRP1 expression had been reported to be stable across age groups[33].

Furthermore, previous studies suggested comparable infection efficacy of primary AECs between children and adults[34]. Notably, in their project, Stolting et al. used primary human respiratory epithelial cells isolated from bronchial brushings. Nasal cells collected here represent upper airway epithelial. Indeed, two studies previously reported differences in SARS-CoV-2 receptor protein expression in a different section of the respiratory tract, which explains differential infection efficacy between studies[32,33].

Gene expression patterns can change in cells and tissues with increasing age and have been associated with changing susceptibility to autoimmune and infectious diseases, including COVID-19[35,36]. This has been linked to changes in epigenetic patterns, particularly DNA methylation[23]. This study links both increased CD13 expression and reduced IFN scores in adults with differential DNA methylation patterns, providing a molecular explanation behind altered gene expression. Increased DNA methylation was seen across *ANPEP* proximal regulatory elements in CYP, which associated with increased DNA methylation within the gene body. Indeed, reduced DNA methylation of regulatory regions, including promoter regions, sufficiently explains increased gene expression[37]. Increased DNA methylation within the gene body can be associated with increased gene expression[37]. Differential methylation of type I IFNs and ISGs in AECs from CYP versus adults also suggests a role of DNA methylation. However, methylation patterns appear more complex when
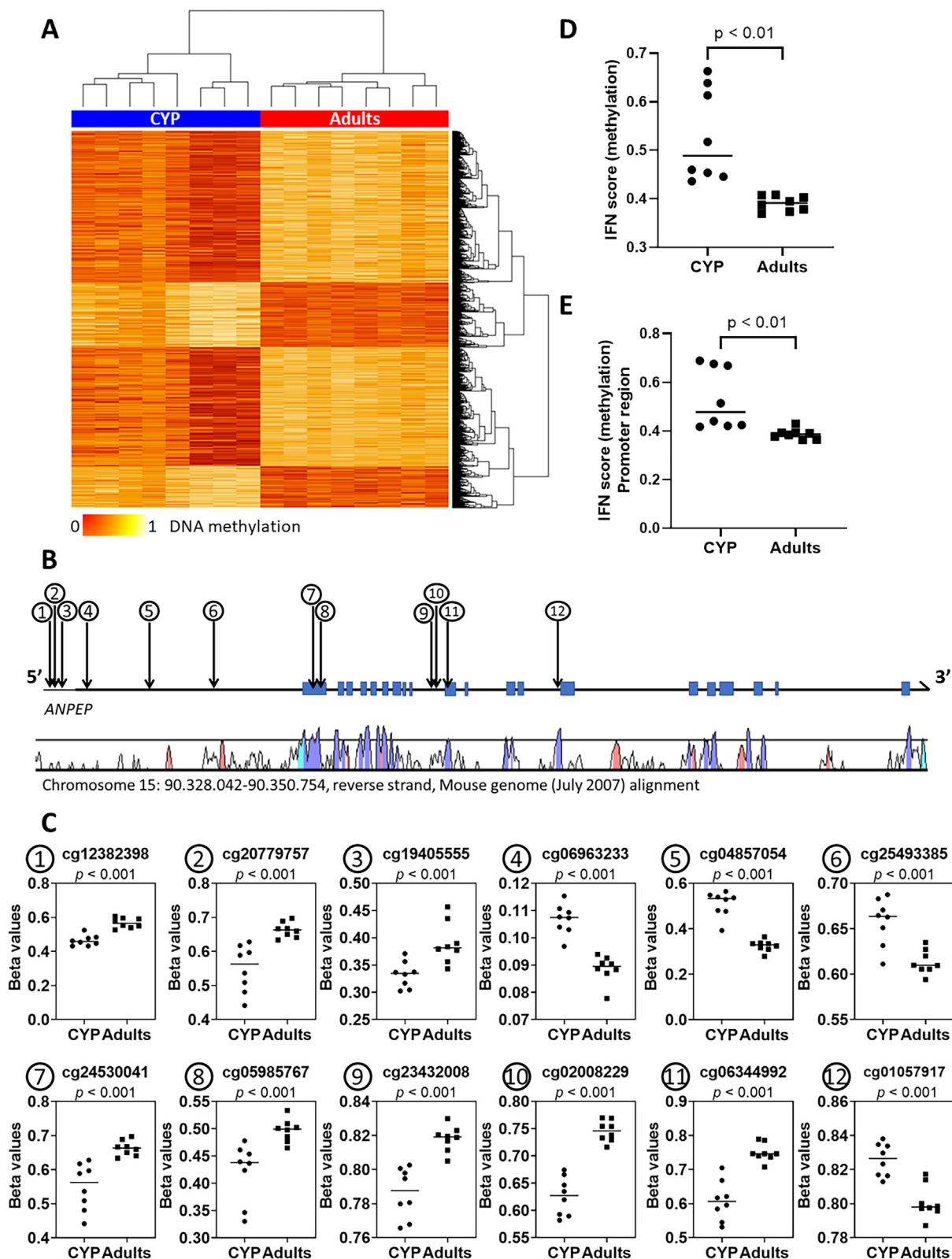
Fig. 4 Differential DNA methylation associates with variable gene expression in airway epithelial cells prior to infection. (A) Heat map showing differentially methylated positions (DMPs) in airway epithelial cells (AECs) from adults and children and young people (CYP) (FDR < 0.01, |Δβ| > 0.1). Red indicates reduced DNA methylation and yellow indicates increased DNA methylation. (B) Map of the *ANPEP* gene displaying 12 differentially methylated positions (DMPs). (C) Beta values of 12 DMPs in *ANPEP* (p-values were corrected for false discovery rates (FDR) and all remained p < 0.001). (D) and (E) Type I IFN methylation scores considering 30 interferon-related genes (Supplementary methods). Significance was calculated using Mann-Whitney tests. CYP = children and young people; IFN = interferons.
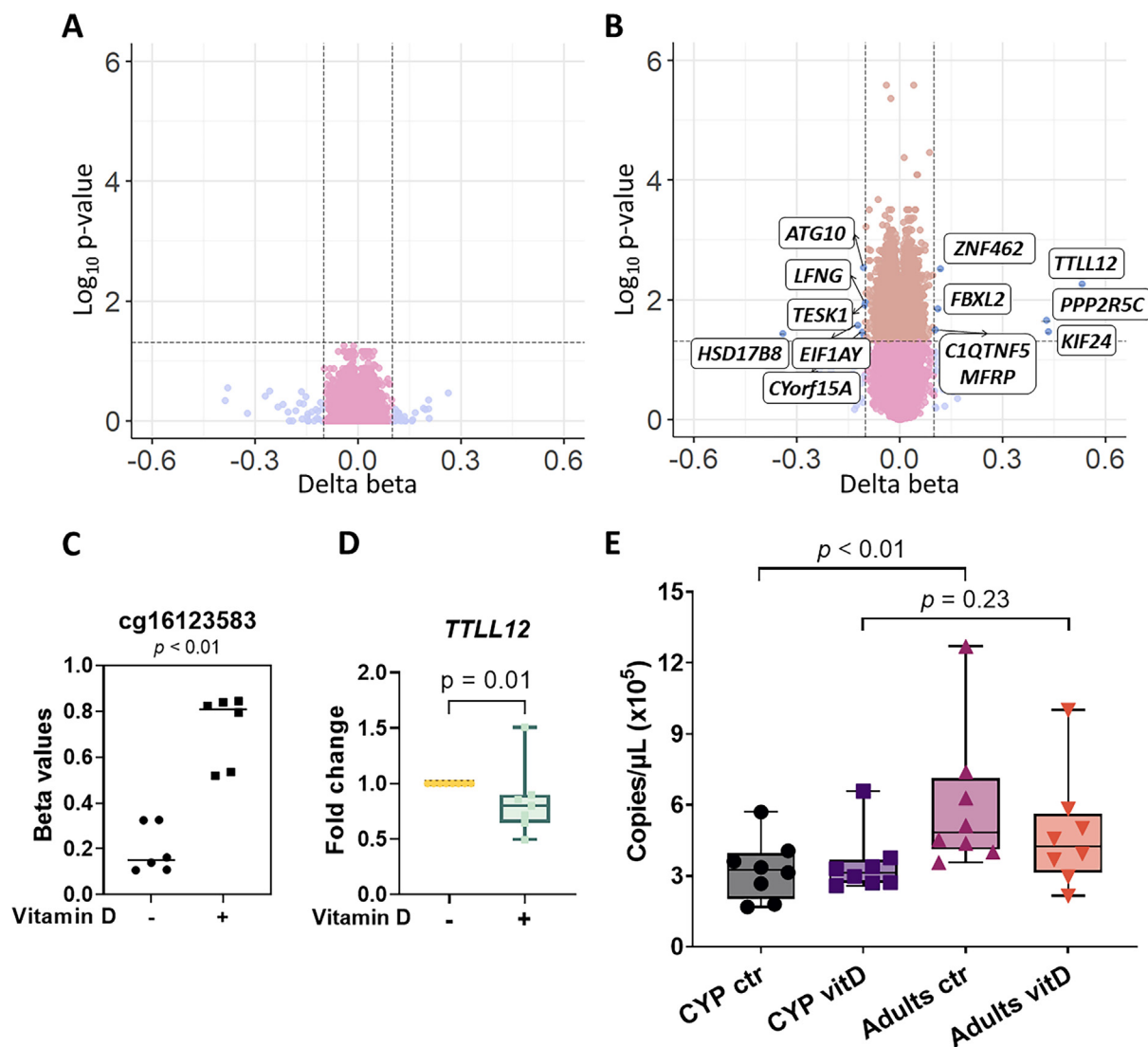
Fig. 5 Vitamin D alters DNA methylation, *TTLL12* expression and viral RNA recovery. (A) and (B) Differentially methylated positions in AECs from CYP (A) and adults (B) in response to vitamin D (p-values were corrected for false discovery rates). (C) Beta values of the CpG located in *TTLL12* in AECs from adult donors in response to vitamin D; (D) Effects of vitamin D on *TTLL12* expression in AECs from adults; gene expression was evaluated via quantitative RT-PCR; fold change is displayed and was calculated as ratio between gene expression in cells treated with vitamin D over cells treated with solvent vehicle; median and interquartile range ($n = 7$). (E) SARS-CoV-2 recovery was quantified using quantitative RT-PCR; median and interquartile range ($n = 8$); significance was tested using the Mann-Whitney test. AEC = airway epithelial cells; CYP = children and young people; RT-PCR = reverse transcription-polymerase chain reaction.

compared to *ANPEP* because regions of increased and reduced methylation coexist[38].

It has previously been suggested that vitamin D modulates immune responses, thereby mediating protection against virus infections[10]. Supportive evidence for this comes from epidemiological studies showing an increased risk of SARS-CoV-2 infection and severe disease in individuals with low vitamin D plasma levels[9,11]. Furthermore, exposure to vitamin D enhances type I IFN responses both in COVID-19 patients and in peripheral blood mononuclear cells *in vitro*[11]. To identify potential molecular mechanisms contributing to protective effects mediated by vitamin D, we exposed AECs from children and adults to vitamin D for four weeks[39]. Supporting preliminary reports, vitamin D exposure resulted in reduced viral RNA recovery in AECs from adults (but not CYP), eliminating age-related differences[8,10].

Because vitamin D has been linked with trans-regulation and epigenetic remodelling of genes relevant to immune responses, we investigated its effect on DNA methylation in AECs[26,27]. Indeed, vitamin D exposure altered DNA methylation of several genes in AECs from adult but not paediatric donors, including *TTLL12*. The *TTLL12* gene encodes for a negative regulator of the innate antiviral RIG-I pathway[25]. RIG-I is a cytoplasmic sensor for RNA viruses that, upon activation, triggers the expression of type I interferons resulting in virus containment and elimination[20]. This study delivers molecular evidence for the involvement of this pathway in vitamin D-mediated effects that provide protection from SARS-CoV-2 infection. The VDR is recruited to *TTLL12* regulatory elements in the proximal promoter where it does not trans-regulate gene expression but co-recruits DNMT1, thereby instructing epigenetic remodelling
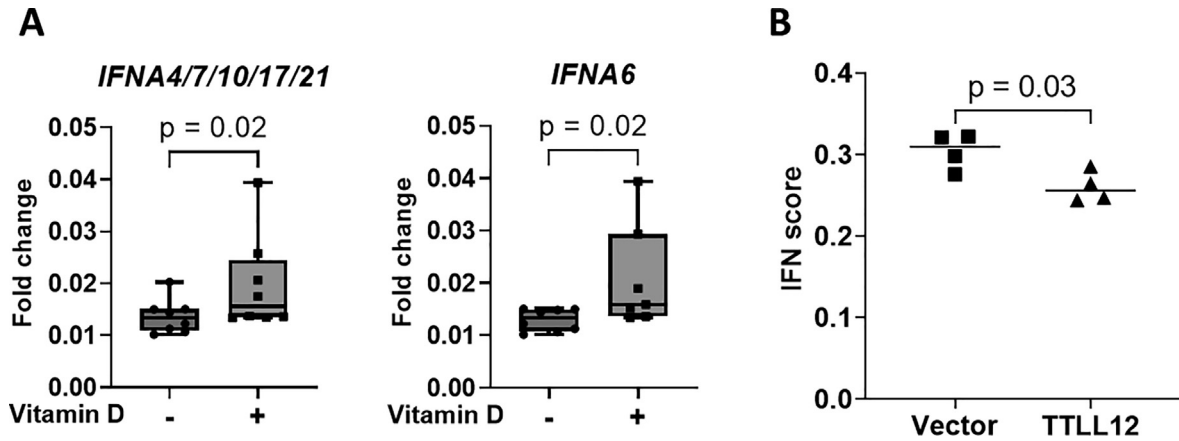
Fig. 6 Vitamin D promotes IFNα expression through silencing of *TTLL12*. (A) Expression of IFNα isoforms, fold change in AECs from adults treated or not treated with vitamin D; statistical significance was tested with the Wilcoxon test (*n* = 8 each); (B) Forced expression of TTLL-12 reduces type I IFN scores; significance was tested using the Mann-Whitney test, data are presented as individual values and median (*n* = 4). IFN = interferon.
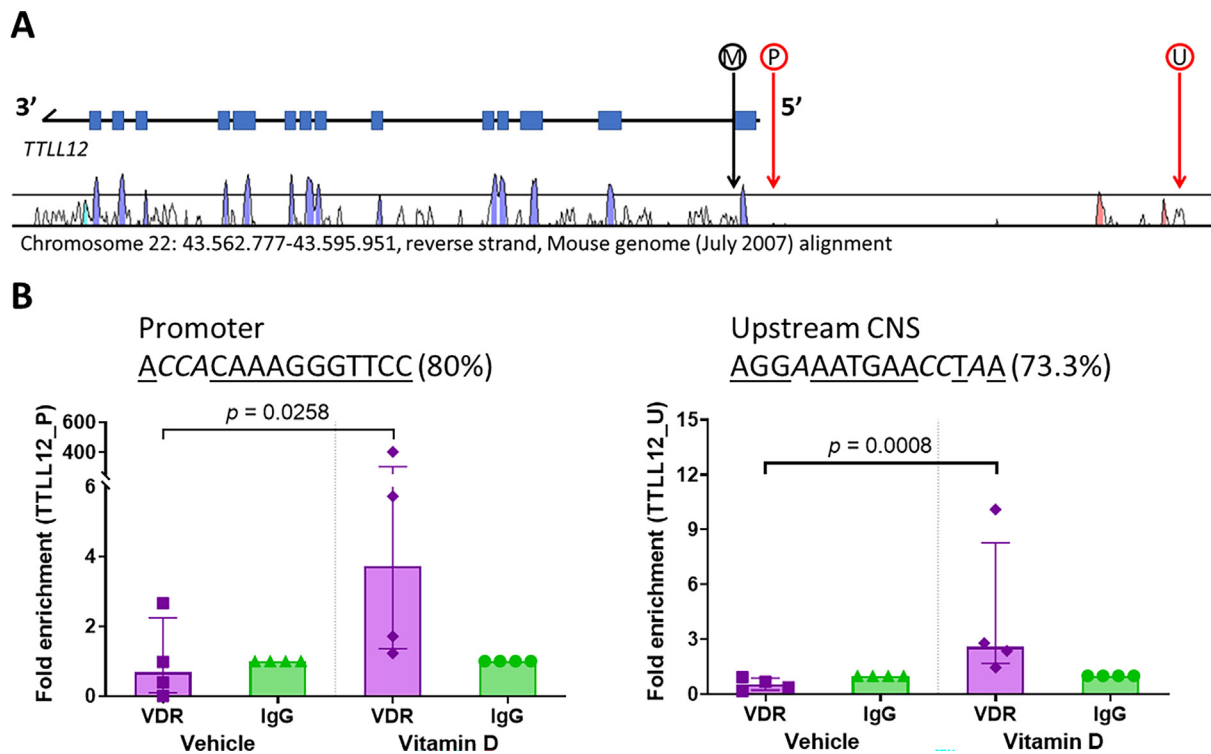
Fig. 7 Vitamin D receptor recruits to *TTLL12*. (A) Map of the *TTLL12* gene, including the differentially methylated CpG (M, cg16123583), a predicted VDR binding element in the proximal promoter (P), and a putative VDR binding site in an upstream CNS region (U). (B) VDR ChIP-qPCR analysis of AECs from adult donors in the presence or absence of vitamin D. Immunoprecipitation with VDR antibodies was normalised against a control IgG; significance was tested using the Kruskal-Wallis test; data are presented as median and interquartile range (*n* = 4). ChIP-qPCR = chromatin immunoprecipitation followed by semi-quantitative polymerase chain reaction; CNS = conserved noncoding sequences; Ig = immunoglobulin VDR = vitamin D receptor.

and silencing of gene expression. Forced expression of TTLL-12 in epithelial cells resulted in reduced type I interferon expression, confirming its role as a suppressor of antiviral responses[25]. Indeed, different studies investigating effects of vitamin D on COVID-19 delivered contrasting results. Although some studies reported that vitamin D did not impact SARS-CoV-2 infection and disease, a large meta-analysis of randomised controlled trials suggested that it reduces RT-PCR positivity rates in individuals exposed to the virus and that it improves disease outcomes[40–42]. Data presented in this manuscript suggest that vitamin D contributes to a reduction of virus recovery through increased type I interferon expression. This supports arguments
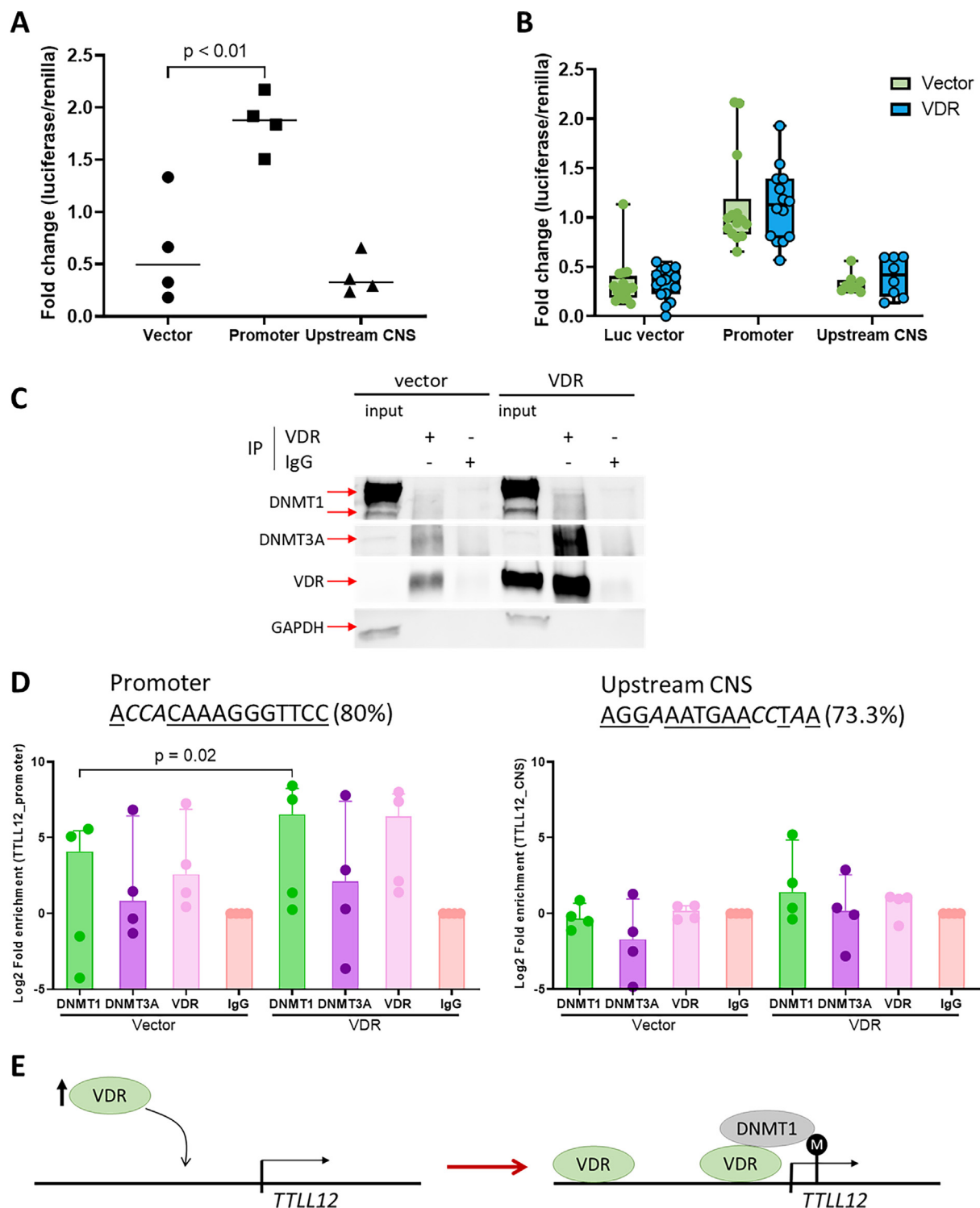
Fig. 8 Vitamin D receptor instructs DNA methylation at *TTLL12*. (A, B) *TTLL12* promoter constructs exhibit increased luciferase activity when compared to empty pGL3 vectors or plasmids including a 5′ CNS region. (B) Forced expression of VDR (as effector) does not alter luciferase activity of the constructs investigated. (C) Co-immunoprecipitation and western blot analysis performed in HEp-2 cells transfected with *VDR* expression plasmids or the empty vectors (pcDNA3.1), using anti-VDR antibodies and IgG controls. Western blots were performed for DNMT1, DNMT3A, VDR and GAPDH. (D) ChIP performed in HEp-2 cells in the absence or presence of VDR overexpression, mapping VDR, DNMT1, and DNMT3A recruitment; statistical significance was tested using the Friedman test; data are presented as median and interquartile range (*n* = 4). (E) Proposed mechanism of VDR-mediated DNA methylation at *TTLL12*. ChIP = chromatin immunoprecipitation; DNMT = DNA methyltransferase ; M = methyl group; VDR = vitamin D receptor.

for prophylactic vitamin D supplementation in adults to protect (somewhat) against virus infections.

While this study identifies age-related differences in AECs, allowing increased infection and virus replication in cells from adults, it has limitations. Because of the complex and time-consuming cell culture system, only a relatively small cohort of donors was accessed (n = 8 per age group), and all individuals had the same ethnic background (White European). Future studies will include samples from additional ethnicities to identify associated differences. Another limitation is the use of panel analyses and not unbiased whole transcriptome and DNA methylome analysis (such as RNA sequencing or RRBS/reduced representation bisulfite sequencing), which may have resulted in oversight of additional differentially regulated genes.

CONCLUSIONS

This study provides evidence for increased SARS-CoV-2 recovery in AECs from adults when compared to children. This partially explains the increased incidences and severity of COVID-19 in adult populations. In addition, AECs from adults exhibit increased expression of CD13, a surface co-receptor promoting coronavirus infection, and reduced spontaneous type I interferon production, an innate antiviral immune mechanism. The study furthermore suggests putative mechanisms behind the potential beneficial effects of vitamin D that amplify anti-viral responses in AECs from adults through the induction of DNA methylation and associated transcriptional suppression of TTLL12, thereby restoring the expression of type I interferons.

METHODS
Cell culture

Primary human AECs were isolated from nasal brushings of healthy donor CYP (<18 years) and adults (>50 years) (Table 1). Cells were co-cultured for one week with mitotically inactivated 3T3-J2F cells, as previously described by Smith and colleagues[17]. AECs were seeded at 150,000 cells/cm^2 on collagen-coated 0.4 μm pore trans-well inserts (cat. 662641, Greiner Bio-One, Frickenhausen, Germany) and grown at the air-liquid interface (ALI) at 37 °C and 5% CO_2 for four weeks to allow their full differentiation. Some cells were cultured with 10^{-9} M 1α,25-Dihydroxyvitamin D_3 (the biologically active form of vitamin D), which represents the estimated physiological concentration in healthy airways (Supplementary Fig. 1), as indicated[43,44]. Vitamin D (cat. D1530, Sigma, Gillingham, UK) was added for the entire culture duration to resemble prolonged physiological exposure and compared to "low" D levels (cultures without addition of vitamin D). Ethanol in the same concentration as in the vitamin D preparation was used as vehicle control (1×10^{-6}%). The absence of pre-existing viral and mycoplasma infection was respectively verified using the Biofire RP2.1 plus platform (bioMérieux, Salt Lake City, UT, USA) or targeted PCR. Cell viability was evaluated each week by measuring transepithelial electric resistance.

HEp-2 cells (ATCC) were cultured in Dulbecco's Modified Eagle Medium (DMEM, cat. 41966029 Gibco, Paisley, UK) supplemented with 10% FBS (cat. 10270106, Gibco, Brazil) and Penicillin-Streptomycin (100 U/mL, cat. 15140-122, Gibco, Paisley, UK) at 37 °C and 5% CO_2.

SARS-CoV-2 infection and viral RNA recovery

AECs were infected with SARS-CoV-2 in vitro. The isolate used (SARS-CoV-2/Human/Liverpool/REMRQ0001/2020) was acquired from nasopharyngeal swabs collected from a patient in Liverpool and passaged a further four times in VERO E6 cells. The viral RNA sequence has previously been submitted to Genbank (Accession No. MW041156). Primary AECs were infected after 28 days of culture at the ALI. The infection was performed at MOI 5 in 200 μL. Cultures were incubated at 37 °C for 48 hours, and supernatants were collected and stored at −80 °C for subsequent RNA extraction. Viral RNA recovery was evaluated using quantitative RT-qPCR of the viral gene Orf-1ab (cat. Z-Path-COVID-19-CE, genesig, Primerdesign, UK).

Gene expression and IFN scores

Total RNA was isolated from AECs and HEp-2 cells using the All-Prep DNA/RNA Mini kit (cat. 80204, Qiagen, Germantown, MD, USA). RNA concentration was then measured using the Qubit (Thermo Fisher Scientific, Waltham, MA, USA).

Gene expression was measured using 100 ng of RNA with the NanoString (NanoString Technologies, Seattle, WA, USA) nCounter Human Host Response Panel at the University of Liverpool Centre for Genomic Research (CGR). Data were normalised and

Table 1. Donor demographics.

Donor	Age	Sex	Ethnicity	Sample group
D28	23 months	M	White European	CYP
D30	10 months	F	White European	CYP
D53	7 months	F	White European	CYP
D54	8 months	M	White European	CYP
D22	10 years	M	White European	CYP
D23	10 years	F	White European	CYP
D26	14 years	M	White European	CYP
D34	12 years	F	White European	CYP
D46	60 years	F	White European	Adults
D49	59 years	M	White European	Adults
D52	64 years	F	White European	Adults
D50	55 years	F	White European	Adults
D51	51 years	F	White European	Adults
D55	55 years	M	White European	Adults
D62	61 years	M	White European	Adults
D9	50 years	M	White European	Adults

CYP = children and young people; F = Female; M = Male.

analysed using R (version 4.2.2) and the NanoStringDiff package (Supplementary methods)[45].

The expression of *TTLL12* was evaluated using Taqman RT-qPCR. RNA was extracted from cells, reverse transcribed into cDNA, and then analysed with Applied Biosystem Taqman probes: TTLL12 Hs00209450_m1 (FAM-MGB) and GAPDH Hs02786624_g1 (FAM-MGB).

IFN scores were calculated using the formula suggested by Tesser *et al.*[22]. Gene counts were normalised to positive and negative controls using the nSolver software (NanoString Technologies, Seattle, WA, USA):

$$IFN\ score = median\left(\frac{Counts\ (genes\ of\ interest)}{Geometric\ mean\ of\ the\ housekeeping\ genes\ counts}\right)$$

A total of 30 IFN-related genes included in the NanoString panel were considered (Supplementary methods).

DNA methylation profiling
DNA was isolated using the AllPrep DNA/RNA Mini kit (cat. 80204, Qiagen, Germantown, MD, USA). DNA methylation profiling was performed on a minimum of 250 ng DNA using Illumina MethylationEPIC BeadChip microarrays (cat. G02090000, Diagenode, Seraing, Belgium). Data were filtered, normalised, and analysed using R (version 4.2.2) as described in the Supplementary methods. IFN scores were calculated using the following formula:

$$IFN\ score = median\ (Beta\ values\ DMPs\ in\ the\ genes\ of\ interest)$$

Immunostaining
AECs grown on transwell inserts for 28 days were fixed with 1% paraformaldehyde (PFA) for 2 hours at room temperature and stored at 4 °C. Cells were rinsed with 1XPBS (Phosphate Buffered Saline) and incubated overnight at 4 °C with 1:300 anti-CD13 (ab7417, Abcam, Cambridge, UK) antibody diluted in 5% FCS 1XPBS. The following day, samples were rinsed three times with 1XPBS and incubated with 1:500 AlexaFluor 488 (cat. A31577, Invitrogen, Thermo Fisher Scientific, Waltham, MA, USA) secondary antibody for 2 hours at room temperature. Cells were then washed and mounted onto a glass slide using DAPI-containing mounting medium (ab104139, Abcam, Cambridge, UK). Immunofluorescence images were taken using the Leica TCS SPE Confocal Microscope, ACS APO 40x/1.15 OIL, and the LAS X acquisition software (Leica Microsystems, Germany), and analysed using ImageJ software (ImageJ, U.S. National Institutes of Health, Bethesda, MD, USA).

Forced expression of genes
Empty pcDNA3.1 plasmid (as a control) and pcDNA3.1 vector carrying the cDNA sequence of *VDR* (Genscript, Accession No: NM_000376.3, Clone ID: OHu25453D) or of *TTLL12* (Genscript, Accession No: NM_015140.4, Clone ID: OHu26655D) were transfected using Lipofectamine2000 (cat. 11668030, Invitrogen, Thermo Fisher Scientific, Waltham, MA, USA) following the manufacturer's protocol.

ChIP
AECs grown on transwell inserts or transfected HEp-2 cells were fixed with 1% PFA for 20 minutes at room temperature, washed twice with 1XPBS, scraped off the membrane, pelleted, and resuspended in 100 μL of lysis buffer supplemented with pro-

tease inhibitors (Invitrogen, Thermo Fisher Scientific, Waltham, MA, USA). Chromatin was fragmented using the Bioruptor Pico Sonicator (Diagenode, Seraing, Belgium). Immunoprecipitation was carried out using the Invitrogen MAGnify Chromatin Immunoprecipitation System (cat. 492024, Thermo Fisher Scientific, Waltham, MA, USA) with anti-VDR (ab109234, Abcam, Cambridge, UK), anti-DNMT1 (PA530581, Thermo Fisher Scientific, Waltham, MA, USA), and anti-DNMT3 (PA1882, Thermo Fisher Scientific, Waltham, MA, USA) antibodies following the manufacturer's protocol. 10% of the sheared chromatin was kept and used as input control. Semi-quantitative PCR was performed with recovered ChIP-DNA using the PrimerDesign PrecisionPLUS qPCR Master Mix (Z-PPLUS-SY-20, Primerdesign, UK) and the following primers: TTLL12 promoter (P) forward 5′-CACTTCTGGCT CCTGTGAGG-3′ reverse 5′-CCCCAACTCATGACTTCTGCT-3′, TTLL12 upstream CNS (U) forward 5′-CCCTGTCAGAGCCTCA CATT-3′ reverse 5′-GGTACACACCTAGTGCACCTC-3′. Data were normalised to the rabbit IgG control. Primers were designed after the identification of putative consensus VDR binding sites within *in silico* identified non-coding sequences conserved across species (CNS) (VISTA genome browser; https://genome.lbl.gov/vista/index.shtml)[26,27,46].

VDR protein co-IP
HEp-2 cells were lysed 17 hours after transfection with pcDNA3.1 empty vector or VDR expression plasmids. Cells were lysed using 200 μL of lysis buffer supplemented with protease inhibitors (cat. 78425, Invitrogen, Thermo Fisher Scientific, Waltham, MA, USA). Co-IP was carried out using the Pierce Crosslink Magnetic IP/Co-IP Kit (cat. 88805, Thermo Fisher Scientific, Waltham, MA, USA) and anti-VDR antibody (ab109234, Abcam, Cambridge), following the manufacturer's instructions. Input lysate and IP samples were analysed via western blotting using the following antibodies: anti-DNMT1 (PA530581, Thermo Fisher Scientific, Waltham, MA, USA), anti-DNMT3A (PA1882, Thermo Fisher Scientific, Waltham, MA, USA), anti-VDR (ab109234, Abcam, Cambridge), and anti-GAPDH (ab8245, Abcam, Cambridge).

Luciferase assays
2.5×10^4 HEp-2 cells were transfected with pGL3 plasmids (empty vectors and plasmids including the *TTLL12* proximal promoter or a 5′ CNS region as indicated) using Lipofectamine2000 (Invitrogen, Thermo Fisher Scientific, Waltham, MA, USA). For some experiments, pcDNA3.1 expression plasmids were added, including the cDNA sequence of *VDR* (Genscript, OHu25453D Accession No: NM_000376.3). The ratio between effector and reporter plasmids was 2.5:1. Each experiment included 0.1 ng of *Renilla* luciferase constructs as an internal control. Five hours after transfection, cells were lysed, and luciferase activity was measured with the Promega Dual Luciferase Assay System (E1910, Promega, Fitchburg, WI, USA) following the manufacturer's instructions.

Data analysis
Gene expression and DNA methylation analyses were performed using R (version 4.2.3) (Supplementary methods). Data were analysed using GraphPad Prism 9 (San Diego, CA, USA) for all other experiments and shown on graphs as individual values or medians with interquartile ranges. As described in figure legends, statistical comparisons were performed with Mann-Whitney, Wilcoxon, Friedman, or Kruskal-Wallis tests.

REFERENCES

1. Gao, Y. D. et al. Risk factors for severe and critically ill COVID-19 patients: a review. *Allergy* **76**, 428–455 (2021).
2. Zhu, N. et al. A novel coronavirus from patients with pneumonia in China, 2019. *N. Engl. J. Med.* **382**, 727–733 (2020).
3. Statsenko, Y. et al. Impact of age and sex on COVID-19 severity assessed from radiologic and clinical findings. *Front. Cell. Infect. Microbiol.* **11**:777070.
4. Ruiz-Aravena, M. et al. Ecology, evolution and spillover of coronaviruses from bats. *Nat. Rev. Microbiol.* **20**, 299–314 (2022).
5. Lim, Y. X., Ng, Y. L., Tam, J. P. & Liu, D. X. Human coronaviruses: a review of virus–host interactions. *Diseases* **4**, 26 (2016).
6. Cantuti-Castelvetri, L. et al. Neuropilin-1 facilitates SARS-CoV-2 cell entry and infectivity. *Science* **370**, 856–860 (2020).
7. Hoffmann, M. et al. SARS-CoV-2 cell entry depends on ACE2 and TMPRSS2 and is blocked by a clinically proven protease inhibitor. *Cell* **181**, 271–280.e8 (2020).
8. Berry, D. J., Hesketh, K., Power, C. & Hyppönen, E. Vitamin D status has a linear association with seasonal infections and lung function in British adults. *Br. J. Nutr.* **106**, 1433–1440 (2011).
9. Ghelani, D., Alesi, S. & Mousa, A. Vitamin D and COVID-19: an overview of recent evidence. *Int. J. Mol. Sci.* **22**, 10559 (2021).
10. Martineau, A. R. et al. Vitamin D supplementation to prevent acute respiratory tract infections: systematic review and meta-analysis of individual participant data. *BMJ* **356**:i6583.
11. Hafezi, S. et al. Vitamin D enhances type I IFN signaling in COVID-19 patients. *Sci. Rep.* **12**, 17778 (2022).
12. Gallagher, J. C. Vitamin D and aging. *Endocrinol. Metab. Clin. North Am.* **42**, 319–332 (2013).
13. Ricci, A. et al. Circulating vitamin D levels status and clinical prognostic indices in COVID-19 patients. *Respir. Res.* **22**, 76 (2021).
14. Merzon, E. et al. Low plasma 25(OH) vitamin D level is associated with increased risk of COVID-19 infection: an Israeli population-based study. *FEBS J.* **287**, 3693–3702 (2020).
15. Ong, L. T. C., Booth, D. R. & Parnell, G. P. Vitamin D and its effects on DNA methylation in development, aging, and disease. *Mol. Nutr. Food Res.* **64**, e2000437 (2020).
16. Gibney, E. R. & Nolan, C. M. Epigenetics and gene expression. *Heredity* **105**, 4–13 (2010).
17. Smith, C. M. et al. Respiratory syncytial virus Increases the Virulence of *Streptococcus pneumoniae* by Binding to penicillin Binding Protein 1a. A new paradigm in respiratory infection. *Am. J. Respir. Crit. Care Med.* **190**, 196–207 (2014).
18. Lachance, C., Arbour, N., Cashman, N. R. & Talbot, P. J. Involvement of aminopeptidase N (CD13) in infection of human neural cells by human coronavirus 229E. *J. Virol.* **72**, 6511–6519 (1998).
19. Nomura, R. et al. Human coronavirus 229E binds to CD13 in rafts and enters the cell through caveolae. *J. Virol.* **78**, 8701–8708 (2004).
20. Crouse, J., Kalinke, U. & Oxenius, A. Regulation of antiviral T cell responses by type I interferons. *Nat. Rev. Immunol.* **15**, 231–242 (2015).
21. McNab, F., Mayer-Barber, K., Sher, A., Wack, A. & O'Garra, A. Type I interferons in infectious disease. *Nat. Rev. Immunol.* **15**, 87–103 (2015).
22. Tesser, A. et al. Higher interferon score and normal complement levels may identify a distinct clinical subset in children with systemic lupus erythematosus. *Arthritis Res. Ther.* **22**, 91 (2020).
23. Wang, K. et al. Epigenetic regulation of aging: implications for interventions of aging and diseases. *Signal Transduct. Target. Ther.* **7**, 374 (2022).
24. Dror, A. A. et al. Pre-infection 25-hydroxyvitamin D3 levels and association with severity of COVID-19 illness. *PLoS One* **17**, e0263069 (2022).
25. Ju, L. G. et al. TTLL12 inhibits the activation of cellular antiviral signaling through interaction with VISA/MAVS. *J. Immunol.* **198**, 1274–1284 (2017).
26. Ramagopalan, S. V. et al. A ChIP-seq defined genome-wide map of vitamin D receptor binding: associations with disease and evolution. *Genome Res.* **20**, 1352–1360 (2010).
27. Pike, J. W. Genome-wide principles of gene regulation by the vitamin D receptor and its activating ligand. *Mol. Cell. Endocrinol.* **347**, 3–10 (2011).
28. Hedrich, C. M. et al. Dynamic DNA methylation patterns across the mouse and human IL10 genes during CD4+ T cell activation; influence of IL-27. *Mol. Immunol.* **48**, 73–81 (2010).
29. Felsenstein, S., Herbert, J. A., McNamara, P. S. & Hedrich, C. M. COVID-19: immunology and treatment options. *Clin. Immunol.* **215**:108448.
30. Felsenstein, S. & Hedrich, C. M. SARS-CoV-2 infections in children and young people. *Clin. Immunol.* **220**:. https://doi.org/10.1016/j.clim.2020.108588 108588.
31. Ho, M. et al. Incidence and risk factors for severe outcomes in pediatric patients with COVID-19. *Hosp. Pediatr.* **13**, 450–462 (2023).
32. Saheb Sharif-Askari, N. et al. Airways expression of SARS-CoV-2 receptor, ACE2, and TMPRSS2 is lower in children than adults and increases with smoking and COPD. *Mol. Ther. Methods Clin. Dev.* **18**, 1–6 (2020).
33. Berni Canani, R. B. et al. Age-related differences in the expression of most relevant mediators of SARS-CoV-2 infection in human respiratory and gastrointestinal tract. *Front. Pediatr.* **9**:697390.
34. Stölting, H. et al. Distinct airway epithelial immune responses after infection with SARS-CoV-2 compared to H1N1. *Mucosal Immunol.* **15**, 952–963 (2022).
35. Hedrich, C. M., Mäbert, K., Rauen, T. & Tsokos, G. C. DNA methylation in systemic lupus erythematosus. *Epigenomics* **9**, 505–525 (2017).
36. Mahmoodpoor, A. et al. Understanding the role of telomere attrition and epigenetic signatures in COVID-19 severity. *Gene* **811**:146069.
37. Moore, L. D., Le, T. & Fan, G. DNA methylation and its basic function. *Neuropsychopharmacology* **38**, 23–38 (2013).
38. Wan, J. et al. Characterization of tissue-specific differential DNA methylation suggests distinct modes of positive and negative gene expression regulation. *BMC Genomics* **16**, 49 (2015).
39. Müller, L., Brighton, L. E., Carson, J. L., Fischer 2nd, W. A. & Jaspers, I. Culturing of human nasal epithelial cells at the air liquid interface. *J. Vis. Exp.* **80**, 50646 (2013).
40. Brunvoll, S. H. et al. Prevention of Covid-19 and other acute respiratory infections with cod liver oil supplementation, a low dose vitamin D supplement: quadruple blinded, randomised placebo controlled trial. *BMJ* **378**, e071245 (2022).

41. Varikasuvu, S. R. et al. COVID-19 and vitamin D (Co-VIVID study): a systematic review and meta-analysis of randomized controlled trials. *Expert Rev. Anti Infect. Ther.* **20**, 907–913 (2022).

42. Jolliffe, D. A. et al. Effect of a test-and-treat approach to vitamin D supplementation on risk of all cause acute respiratory tract infection and Covid-19: phase 3 randomised controlled trial (CORONAVIT). *BMJ* **378**, e071230 (2022).

43. Brockman-Schneider, R. A., Pickles, R. J. & Gern, J. E. Effects of vitamin D on airway epithelial cell morphology and rhinovirus replication. *PLoS One* **9**, e86755 (2014).

44. Greiller, C. L. et al. Vitamin D attenuates rhinovirus-induced expression of intercellular adhesion molecule-1 (ICAM-1) and platelet-activating factor receptor (PAFR) in respiratory epithelial cells. *J. Steroid Biochem. Mol. Biol.* **187**, 152–159 (2019).

45. Wang, H. et al. NanoStringDiff: a novel statistical method for differential expression analysis based on NanoString nCounter data. *Nucleic Acids Res.* **44**, e151 (2016).

46. Hedrich, C. M. & Bream, J. H. Cell type-specific regulation of IL-10 expression in inflammation and disease. *Immunol. Res.* **47**, 185–206 (2010).